Available online at www.sciencedirect.com
SCIENCE DIRECT®
Journal of Nuclear Materials 337–339 (2005) 310–314
journal of nuclear materials
www.elsevier.com/locate/jnucmat

Kinetic investigation of a collisionless scrape-off layer with a source of poloidal momentum

J.P. Gunn *

Association Euratom-CEA, CEA/DSM/DRFC, Centre de Cadarache, F-13108 Saint Paul Lez Durance, France

Abstract

The influence of a source of poloidal momentum on the collisionless tokamak scrape-off layer (SOL) is investigated. The solutions of the kinetic equation for ion flow and the corresponding system of fluid equations assuming zero ion heat flux are compared. The two models agree quite well for small poloidal Mach numbers of the momentum source, and for larger Mach numbers near the target towards which the drift is directed. At the other target the agreement is poor because the kinetic heat flux dominates energy transport near the stagnation point. The kinetic model yields smooth solutions for any value of poloidal drift. The fluid model breaks down at a particular supersonic poloidal Mach number due to the appearance of a singularity on the domain. The failure of the fluid model does not represent a real detachment, but is simply a mathematical artefact caused by the truncation of the series of fluid moment equations.

PACS: 52.25.Dg; 52.30.−q; 52.40.Hf; 52.65.−y
Keywords: Edge modelling; Kinetic effects; Plasma flow

1. Introduction

Simple one-dimensional (1D) analysis of the tokamak scrape-off layer (SOL) is valuable in that it gives intuitive insight into the complex phenomena that can occur [1]. Despite their obvious usefulness for validating fluid models, kinetic solutions of the simple SOL problem are rare [2], and none exist for the problem with poloidal drifts. This problem is of interest because even a small poloidal drift having low Mach number can compete with the poloidal projection of sonic parallel flow at the plasma-sheath interface [3]. Simple considerations have led to the formulation of the Bohm–Chodura boundary condition which states that the poloidal projection of the fluid velocity must be at least equal to the poloidal projection of the parallel ion sound speed [4]. As a result the parallel flow speed is supersonic for a drift directed away from the target, and subsonic for a drift directed towards the target. This seems to cause problems for 2D fluid codes, however, and ad hoc boundary conditions are sometimes imposed in order to circumvent numerical problems. Given the importance of the boundary conditions in determining the overall behaviour of the SOL, it is clearly of interest to delve into the basic physics governing this problem. Chung and Hutchinson [5] solved the kinetic equation for a Mach probe in a semi-infinite plasma with parallel flow, and confirmed the results of a simpler isothermal fluid calculation. In Section 2 of this paper we will apply their collisionless kinetic equation to the bounded SOL

* Tel.: +11 33 4422 57902; fax: +11 33 4422 54990.
E-mail address: jamie.gunn@cea.fr

0022-3115/$ - see front matter © 2004 Published by Elsevier B.V.
doi:10.1016/j.jnucmat.2004.10.054

with drifts. The solution of the corresponding fluid mass, momentum, and energy transport equations is described in Section 3. The kinetic and fluid solutions are compared in Section 4, with particular attention paid to the boundary conditions. The main results are summarized in Section 5.

2. Kinetic model

All the physical quantities appearing in this paper are expressed in dimensionless units (see Table 1). The SOL is treated as a thin slab interfacing via a magnetic separatrix to a semi-infinite, spatially uniform source plasma. The system is bounded by two target plates separated by poloidal length L_θ. The magnetic field lines lie in the ϕ–θ plane making an angle α with the toroidal direction. The toroidal gradients are zero. Radial gradients will be approximated by source terms. We seek the equilibrium poloidal profile of the phase space density $f(x_\theta, v_\theta)$ which is governed by the stationary collisionless Vlasov equation

$$v_\theta \frac{\partial f}{\partial x_\theta} + E_\theta \frac{\partial f}{\partial v_\theta} = W(x_\theta)[f_0(v_\theta, V_R) - f(x_\theta, v_\theta)]. \quad (1)$$

The ion speed is the sum of the poloidal projections of the parallel velocity (unique to each ion) plus a perpendicular drift velocity (the same for all ions) $v_\theta = v_\parallel \sin\alpha + V_\perp \cos\alpha$, where $V_\perp$ could be a poloidal $\vec{E}_r \times \vec{B}$ drift. Quasineutrality is imposed, and the self-consistent poloidal electric field is given by the Boltzmann relation for isothermal electrons $E_\theta = -(\mathrm{d}n/\mathrm{d}x_\theta)/n$. We make this approximation in order to be able to compare with the equivalent fluid model later on, and in any case it is reasonable to neglect the sheath which can usually be considered as sourceless, collisionless, and very thin in tokamaks (sheath thickness $\sim$0.1 mm compared to poloidal circumference $\sim$5 m). We adopt the volumetric source term of Chung and Hutchinson [5] where $f_0(v_\theta, V_R)$ is a shifted Maxwellian distribution with temperature T_0

Table 1
Normalization of the pertinent physical quantities

Physical quantity	Normalization (MKS units)
Electric charge	Unit charge e (1.6×10^{-19} C)
Mass	Ion mass m_i (kg)
Energy	Source electron thermal energy kT_e (J)
Distance	Poloidal length L_θ (m)
Speed	Poloidal projection of cold ion sound speed $c_e = \sqrt{kT_e/m_i}\sin\alpha$ (m s^{-1})
Time	Poloidal ion transit time $L_\theta/c_e \sin\alpha$ (s)
Density	Source plasma density n_0 (m^{-3})

$$f_0 = \frac{1}{\sqrt{2\pi T_0}} \exp\left(-\frac{(v_\theta - V_R)^2}{2T_0}\right). \quad (2)$$

The key parameter in this study is what we call the 'relative' poloidal speed $V_R = V_{\parallel 0}\sin\alpha + V_\perp \cos\alpha$ of the source plasma with respect to the target plates, where $V_{\parallel 0}$ is an arbitrary parallel drift speed of the source plasma. It is easy to see that the solution of Eq. (1) $f(x_\theta, v_\theta)$ in a phase space (x_θ, v_θ) in which we absorb the drift component $V_\perp \cos\alpha$ into the source term $f_0(v_\theta, V_R)$ is identical to $f(x_\theta, v_\parallel \sin\alpha)$ in which the source term would be $f_0(v_\parallel, V_{\parallel 0}\sin\alpha)$ and the SOL poloidal drift is explicitly accounted for by shifting the characteristics along the $v_\parallel$-axis by an amount $-V_\perp \cos\alpha$. There is no difference between the influence of a momentum source due to a poloidal drift in the SOL, and viscous coupling with a parallel flow in the core plasma (at least in slab geometry). The source term represents the exchange of ions between the two regions at a characteristic frequency $W(x_\theta)$ that can have an arbitrary spatial variation and satisfies $\int_{-L_\theta/2}^{L_\theta/2} \mathrm{d}x_\theta W(x_\theta) = 1$. Allowing the frequency to vary in space is a convenient alternative to non-linear grid spacing. In the usual case when $W = 1$, as imposed by our choice of normalization, the spatial derivatives of all the fluid quantities become formally infinite at the boundaries, and using a variable grid spacing is one way to deal with the numerical difficulties near the singularities. On the other hand, keeping a uniform spatial grid but choosing $W(x_\theta = \pm L_\theta/2) = 0$ eliminates the singularity and allows the solution to proceed gently to the wall with all gradients tending to zero. For this study we use $W(x_\theta) = 1 + \cos(2\pi x_\theta)$. This is equivalent to a coordinate transformation. After the solution is obtained, it is simple to map x_θ into a space x'_θ where $W = 1$: $\int_{-L_\theta/2}^{x'_\theta} \mathrm{d}x'_\theta = \int_{-L_\theta/2}^{x_\theta} \mathrm{d}x_\theta W(x_\theta)$. We take the sign of V_R to be positive and refer to the target at $x_\theta = +L_\theta/2$ towards which the drift is directed as 'active', and the other one at $x_\theta = -L_\theta/2$ as 'inactive'. The solution of Eq.(1) begins by imposing an E_θ with the following properties. Near the inactive target $E_\theta < 0$ and near the active target $E_\theta > 0$, consistent with ion acceleration from a stagnation point somewhere in the SOL. At both targets $E_\theta = 0$ because of our choice of $W(x_\theta)$. The characteristics of motion along which f is convected describe the ion trajectories through phase space. Eq. (1) is integrated starting at one of the targets as time advances. The initial conditions are $f(x_\theta = -L_\theta/2, v_\theta > 0, t = 0) = 0$ and $f(x_\theta = +L_\theta/2, v_\theta < 0, t = 0) = 0$. The integration is carried forward until the characteristic intersects one of the targets (Fig.1). Roughly 500–1000 characteristics must be integrated in order to sufficiently map out f. The point where E_θ changes sign is the X-point of a separatrix. Ions never move from the X-point and at equilibrium the solution there is simply $f = f_0$. A characteristic that originates from the inactive target will return there if its initial speed lies below the upper branch of the

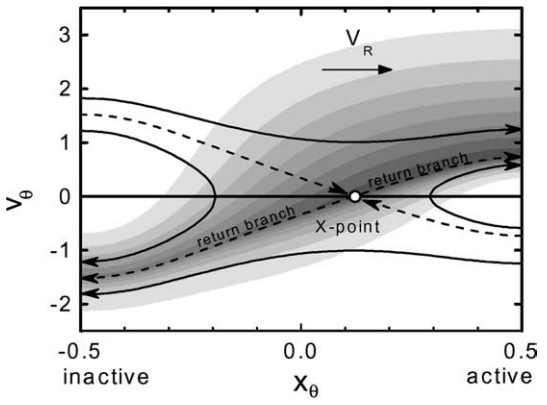

Fig. 1. The gray shading indicates contours of constant f for $T_0 = 2$, $V_R = 1$. There are eight equally spaced contour levels between $f = 0$ (white) and the maximum value for this case $f = 0.227$ (dark gray). The active target is the one towards which is V_R directed. The maximum n occurs at the X-point where $v_\theta = 0$ and $E_\theta = 0$. In this particular case the stagnation point of the poloidal fluid flow $\langle v_\theta \rangle = 0$ lies at $x_\theta = -0.14$. The four classes of characteristics (full curves) and the separatrix (dashed curve) are shown.

separatrix. Otherwise it terminates on the opposite target. The characteristics that are the branches of the separatrix itself only intersect one target; they approach the X-point asymptotically. The branch that starts at the X-point and flows towards the targets has special properties; we refer to it as the 'return branch'. The n is calculated on a regular spatial grid with typically 100–200 points to obtain E_θ^*. The E_θ used for iteration i is relaxed to the next iteration $i+1$ following the scheme $E_\theta^{i+1} = (1-\varepsilon)E_\theta^i + \varepsilon E_\theta^*$ where we take $\varepsilon = 0.05$. The calculation converges after about 30 iterations.

The general features of the solution are illustrated in Fig. 1 for $T_0 = 2$ and $V_R = 1$. The X-point where n peaks is driven towards the active target by the asymmetry of the source. The poloidal stagnation point where $\langle v_\theta \rangle = 0$ lies somewhere between the inactive target and the X-point except for the symmetric case $V_R = 0$ when the stagnation point and the X-point coincide. For supersonic V_R most of the ions are born with such large v_R that their characteristics are only slightly deviated by the E_θ; the active target distribution is similar to the one that would arise from a ballistic calculation where $E_\theta = 0$ and all the characteristics are horizontal lines. There are always some ions born in the wings of the source distribution. Those ions populate the longest characteristics that flow from the inactive target to the X-point and back again and give rise to a narrow stream near the return branch of the separatrix. There appears to be no limit to the magnitude of V_R. As V_R is increased, n drops because the average dwell time in the SOL becomes very short. The X-point moves asymptotically close to the active target, but never actually touches it. Likewise, the stagnation point moves towards the inactive target. In contrast to the prediction of the simplified fluid model, smooth solutions are obtained for all values of V_R; no evidence of sudden detachment [1, p. 552] nor any abrupt change in the qualitative nature of the solution appears. In the next section we develop the system of exact fluid equations that describes this physical model.

3. Fluid model

Taking the first three moments of Eq. (1) we obtain the following system of fluid equations for n, the poloidal flow speed V_θ, and the kinetic 'temperature' T:

$$\frac{dn}{dx_\theta} = W\frac{3V_\theta^2 - 3V_R V_\theta + V_R^2 - 3T + T_0 + n(2T - V_\theta^2)}{V_\theta(V_\theta^2 - 1 - 3T)}, \tag{3}$$

$$\frac{dV_\theta}{dx_\theta} = W\frac{n(1+T) - 1 - T_0 - (2V_\theta - V_R)(V_\theta - V_R)}{n(V_\theta^2 - 1 - 3T)}, \tag{4}$$

$$\frac{dT}{dx_\theta} = W\frac{[T_0 + (V_\theta - V_R)^2](V_\theta^2 - 1) + [(3-2n)(1+T) - V_R^2 - T_0]T}{nV_\theta(V_\theta^2 - 1 - 3T)}, \tag{5}$$

where we set the ion heat flux density $q = n\langle (v_\theta - V_\theta)^3 \rangle / 2 = 0$. The term in parentheses in each of the denominators is the Bohm–Chodura singularity. We divide the n and T equations by the V_θ equation to eliminate x_θ. The two new equations for $n(V_\theta)$ and $T(V_\theta)$ are integrated starting at the poloidal stagnation point $V_\theta = 0$, which is also a singularity. The only way that n and T can be finite and continuous there is if the numerators tend to zero. That condition imposes a relationship between those two quantities. For a chosen initial n, the corresponding T is uniquely determined, and the initial slopes can be obtained using l'Hôpital's rule. The equations are integrated towards both targets until the Mach number $M_\theta = V_\theta/\sqrt{1+3T}$ becomes unity. The flow equation is then inverted to solve for $x(V_\theta)$. The initial n and T must be chosen such that $L_\theta = 1$, with the Bohm–Chodura singularities lying precisely at the targets. These two boundary conditions, plus the requirement of smooth profiles, are the three physical constraints that determine the unique solution. They cannot be chosen freely, but are furnished by the fluid equations themselves [6]. The solution procedure involves iterating to find the correct stagnation point pressure that makes the final solution fit between the targets. The present solution differs slightly from the bounded isothermal SOL model of Hutchinson [7] in which he imposed a value for the density at a specific point and calculated the resulting system length as a variable.

When the numerator of Eq. (4) becomes zero, a singularity appears in the SOL and the fluid solution breaks down. This occurs for large V_R. This is the same sort of singularity that causes the simple isothermal fluid model to fail. In that case, its occurrence (at $V_R = 2.0$) coincides with the disappearance of n from the inactive target, leading to the speculation that some sort of abrupt detachment occurs [1, p. 552]. In the case of the 3-moment equations all the plasma parameters remain finite and solutions can be found until much higher V_R, for example up to $V_R \simeq 4$ with $T_0 = 2$. We propose that this limit has no physical significance but is rather a mathematical artefact caused by the truncation of the series of fluid equations. Presumably if higher fluid moments were retained, the range of V_R for which solutions can be found would increase. Given an arbitrarily large V_R, there is no physics in this one-dimensional, collisionless model that prevents stable solutions from existing. Whether or not such large values of drift really occur self-consistently in tokamaks needs to be addressed by fully two-dimensional calculations including electric current circulation.

4. Comparison of kinetic and fluid calculations

Poloidal profiles calculated by the kinetic and fluid equations are compared in Fig. 2 for $T_0 = 2$ and for $V_R = 0$ and 1.6. The plasma parameters at the targets, denoted by subscript 't' are shown in Fig. 3 as a function of V_R. The solutions behave the same way for other values of T_0. Let us summarize the main features of the kinetic results and the differences between them and the fluid results.

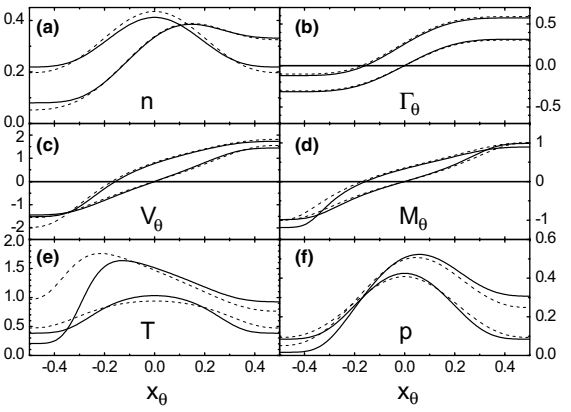

Fig. 2. Poloidal profiles of normalized (a) density, (b) poloidal flux, (c) poloidal flow speed, (d) poloidal flow Mach number, (e) ion temperature, and (f) ion pressure for source temperature $T_0 = 2.0$ calculated by kinetic (full curves) and fluid (dashed curves) models. The curves that are symmetric and asymmetric with respect to $x_\theta = 0$ correspond respectively to $V_R = 0$ and 1.6.

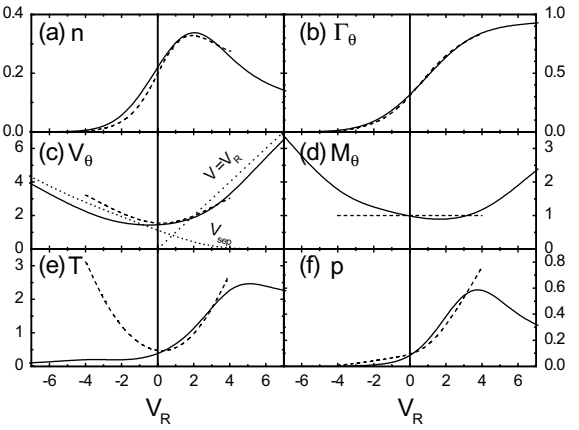

Fig. 3. Normalized target plate plasma parameters as a function of poloidal drift V_R for $T_0 = 2.0$. The display scheme is the same as Fig. 2. In panel (c), the separatrix speed and the drift speed are indicated by dotted curves.

When $V_R = 0$ the SOL is poloidally symmetric about $x_\theta = 0$. n decreases by roughly 1/2 between the stagnation point and the targets due to the acceleration of the ions. When a source of momentum is present ($V_R \neq 0$) the density peak is pushed towards the active target and the stagnation point towards the inactive target. For moderate V_R the inactive n_t decreases while increasing at the active target. For supersonic V_R the active n_t rolls over and decreases steadily due to the smaller ion dwell time. The kinetic and fluid calculations agree quite well, although n is slightly underestimated near the inactive target.

The effect of V_R on the flux Γ_θ is simply to offset the poloidal profile with relatively little change of its overall shape. For large V_R when the stagnation point is just in front of the inactive target, almost all the flux goes to the active target. The kinetic and fluid calculations agree almost perfectly for all V_R.

For low V_R the classical picture of ion acceleration up to the sound speed is roughly confirmed by the kinetic calculations. The fluid V_t is somewhat higher than the kinetic value near the inactive target for large V_R but in good agreement everywhere else in the SOL. Kinetic effects govern V_t at supersonic V_R beyond which the fluid solutions break down. At the active target we have $V_t \to V_R$. Onto the inactive target flows a cold beam of ions along the return branch of the separatrix. Their speed is therefore largely determined by the poloidal density gradient via Boltzmann's relation. It should be stressed here that we are modelling the *total poloidal flow speed* which includes the poloidal drift plus the parallel flow. To obtain the parallel flow from these results one just has to subtract V_R from V_θ. For large negative V_R

the parallel flow becomes hypersonic. This does not pose any problem at all, even for the fluid model.

This comparison is of particular interest because we are in effect calculating the true fluid boundary conditions as a simple output of the kinetic model, and comparing with the theoretical fluid Mach number as extracted from the target plate singularities. In order to have a familiar point of reference we have calculated the local ion sound speed from the kinetic T profiles to define a Mach number $M_\theta = V_\theta/\sqrt{1+3T}$. For low to moderate V_R, in the SOL and near the active target the kinetic and fluid calculations agree fairly well although the kinetic M_θ is slightly less than 1. In all other conditions it is very large. The kinetic effects mentioned in the previous paragraph dominate.

For low V_R the T_t is lower than in the SOL due to the acceleration. Both kinetic and fluid models agree in that V_R pushes the n peak towards the active target, while pushing the T peak towards the inactive target. As V_R increases, T_t at the active target increases and saturates close to T_0. The fluid model reproduces the increase, but not the saturation which is a kinetic effect. At the inactive target, however, for all V_R, the fluid model fails completely. The kinetic model predicts a continuous decrease of T_t whereas the fluid model gives the opposite. The low kinetic T_t is the origin of the high M_θ.

The kinetic pressure behaves like n. The agreement between the fluid and kinetic calculations is poorer due to the problems with T.

5. Discussion and conclusion

The kinetic equation that we solve is mathematically identical to that of Chung and Hutchinson [5]. What is new here is its application to a bounded SOL, the demonstration of the equivalence between the two types of momentum source, and the detailed comparison with the fluid equations. The fluid model is quite faithful to the kinetic model in the SOL and near the active target for low to moderate V_R (i.e. for values that are observed in tokamaks). However, it breaks down near the inactive target. By identifying the main features of the kinetic solution in this region we can hope to gain some insight into why the two models disagree so strongly. The three components of the total ion energy flux density $n\langle v_\theta^3\rangle/2 = q + 3V_\theta p/2 + nV_\theta^3/2$ are shown in Fig. 4 for $V_R = 1.6$. q is relatively small near the active target where the agreement is good, but it dominates in the vicinity of the energy flux stagnation point $\langle v_\theta^3\rangle = 0$ where the kinetic and fluid models diverge from one another. By definition q carries 100% of the power flux at the flow stagnation point $\langle v_\theta\rangle = 0$. If we were to expand our fluid hierarchy to include higher order transport equations, maybe better agreement would be found. Furthermore, with each new equation, the Bohm–Chodura singularity would evolve to take account of the higher moments, and perhaps the Mach number derived from the kinetic solution would tend to unity over a broader range of V_R. For example, the determinant of the system that includes the heat flux transport equation gives rise to a more refined version of the Bohm–Chodura singularity $nV^4 - nV^2 + 8Vq - 3p = 0$ which reduces to the more familiar 3-moment singularity in the limit of small q. We note that the poloidal momentum source, whether it is provided by SOL cross-field drifts or viscous coupling with parallel flow in the core, does not explicitly affect the boundary conditions for the total poloidal flow in the sense that it does not appear in the ion sound speed as defined by the singularity. The reason is that the poloidal drift V_R appears only in the source terms; it is completely dissociated from the poloidal divergence terms in the equations.

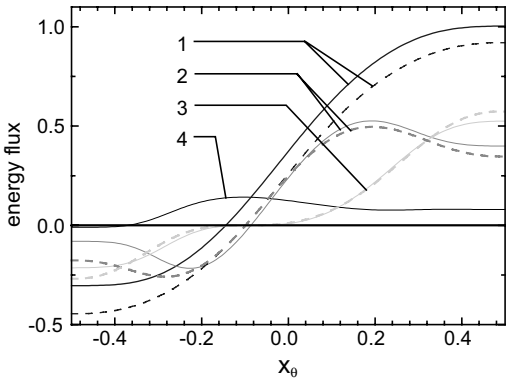

Fig. 4. The kinetic (full curves) and fluid (dashed curves) components of the poloidal energy flux for $T_0 = 2$, $V_R = 0.8$. (1) total energy flux $n\langle v_\theta^3\rangle/2$; (2) pressure convection $3V_\theta p/2$; (3) kinetic energy convection $nV_\theta^3/2$; (4) heat flux $q = n\langle(v_\theta - V_\theta)^3\rangle/2$. The fluid heat flux is forced to zero.

Acknowledgments

I thank Dr Vladimir Fuchs and Dr Thierry Loarer for helpful discussion.

References

[1] P.C. Stangeby, The Plasma Boundary of Magnetic Fusion Devices, Institute of Physics, Bristol and Philadelphia, 2000.
[2] R.C. Bissel, P.C. Johnson, P.C. Stangeby, Phys. Fluids B 1 (1989) 1133.
[3] E. Gravier, J.P. Gunn, J.-L. Lachambre, et al., Nucl. Fus. 42 (2002) 653.
[4] V. Rozhansky, M. Tendler, Phys. Plasma. 1 (1994) 2711.
[5] K.-S. Chung, I.H. Hutchinson, Phys. Rev. A 38 (1988) 4721.
[6] R.H. Cohen, D. Ryutov, Phys. Plasmas 6 (1999) 1995.
[7] I.H. Hutchinson, Phys. Fluids B 3 (1991) 847.